

Passive Attenuation to Allow Muon Calibration of NuLat Detector

Andrew Gunsch, Coe College, Department of Physics

Mentor: Dr. Bruce Vogelaar, Virginia Tech, Center for Neutrino Physics

24 July, 2019

Abstract

The Neutrino Lattice Experiment (NuLat) is a novel neutrino detector made of 125 scintillating cubes. Due to its unique geometry, it is able to observe the topology of signals. Before data can be collected, the NuLat detector must be calibrated. One approach is calibrating to muon signals, for the average energy deposited by muons in a plastic scintillator is well-documented. The detector was designed to collect positron and neutron capture signals from the Inverse Beta Decay of an antineutrino, so the higher-energy signals from muons would saturate the detector, clipping the signals and rendering the amplitudes unmeasurable. We built resistive pads to attenuate the signals from two of the detector's faces. These passive attenuators did not need to be symmetric, so they were assembled in the voltage divider configuration. The pads lowered the amplitude of the signals to a tenth of their initial levels. Then we used a Fortran algorithm to simulate muons propagating vertically through the detector. The simulated data was compared to the muons detected experimentally. The photomultiplier tube responses for similar events were comparable on the attenuated faces, but there was still saturation in the face that was not attenuated. Attenuating the signals shows promise for enabling muon calibration of NuLat. In the future, the detector will need two voltage ranges. There must be an attenuated range for measuring the signals from muons and a non-attenuated range for measuring the signals from the decay of antineutrinos.

1. Introduction

For decades, the Standard Model of particle physics has been used as the basis for theory and experimentation in the field. This model groups all of the truly fundamental particles of reality into three categories, as follows: six quarks, six leptons, and six bosons. The bosons are carriers of the four fundamental forces, by which the quarks and leptons (collectively known as “fermions”) interact. The fermions also have anti-matter counterparts.

The set of twelve fermions are additionally split into three generations. The first-generation lepton is the electron. Next is the more massive muon, and finally the most massive known lepton: the tau. All three carry negative charge. The model also includes three other leptons. These are the chargeless neutrinos. Neutrinos are linked to the charged leptons through their flavor eigenstates. There is an electron neutrino, a muon neutrino, and a tau neutrino^[1].

Neutrinos may be an avenue for discovering physics beyond the Standard Model. When a flux of neutrinos is observed at its source and at a destination, the proportion of each flavor to the whole will usually appear different. For example, the Sun produces electron neutrinos through its proton-proton chain processes, but when solar neutrinos are detected on earth, a large portion of them are observed as muon neutrinos^[1]. The earliest evidence of this phenomenon was found by the Homestake experiment in the 1960s, in which only 30% of the expected solar neutrino flux was detected^[1]. Similar findings by other solar neutrino experiments over the subsequent

decades, such as Super Kamiokande, corroborated these anomalous findings, resulting in the theory of neutrino oscillation.

The current understanding of this neutrino oscillation phenomenon is that the neutrino flavor eigenstate is a superposition of mass eigenstates. Likewise, the neutrino mass eigenstate is theorized to be the superposition of the flavor states. This theory clearly mandates that neutrinos have mass, but according to the Standard Model, they should not, providing evidence for physics beyond the Standard Model^[2]. Additionally, investigations into neutrino oscillation have discovered peculiar oscillations that violate the presumed rules of the phenomenon^[1]. This has led to suspicion that a fourth, flavorless neutrino exists: the so-called “sterile neutrino”. Further study of neutrinos is needed to explore these various avenues to physics beyond the Standard Model.

2. Design of the NuLat Detector

The NuLat detector is a novel particle detector that is comprised of plastic scintillating cubes. The cubes are arranged in a 5 x 5 x 5 Raghavan Optical Lattice (ROL), with 125 cubes in total. By using cubes in an ROL, there is total internal reflection in the gaps between the cubes, so the light transmitted from cube to another keeps moving in the same direction, so light scattering isn't too common^[1]. It is intended primarily for detecting antineutrinos through the Inverse Beta Decay reaction.

As is often true in particle physics, the only way to detect the presence of an electron antineutrino is to destroy it. Through the Inverse Beta Decay (IBD), an electron antineutrino weakly-interacts with a proton, and produces a neutron and a positron. The weak interaction in this case is carried by the W^- boson. The energy of the proton, compared to that of the antineutrino, is negligible. Therefore, when the interaction occurs, the energy and momentum from the antineutrino is split between the neutron and the positron. Most of the energy goes to the positron, and most of the momentum goes to the neutron^[1]. The IBD interaction releases a Q-value of 1.8 MeV^[2].

It is easy to detect a signal from the positron. As quickly as it comes into existence, it annihilates with an electron, producing two gamma rays, each of energy 0.511 MeV, which the detector's cubes can easily catch. The neutron, as it moves away from the positron, will be captured by the scintillating cubes. The cubes in the central 3 x 3 x 3 lattice are doped with Lithium-6 to facilitate neutron capture. Lithium-6 has a large neutron cross-section, so it is likely that the neutron will interact with it. After capturing the neutron, the newly-formed Lithium-7 isotope quickly decays into an alpha particle and tritium, while releasing 4.8 MeV of energy, which the photomultiplier tubes can detect.

Antineutrino IBD events are best identified by observing both the capture of a quenched neutron and the annihilation of a positron. The scintillating cells of NuLat facilitate the identification of this particular topology, enabling easier analysis of these events. After passing through light guides, the scintillating light from a particle interaction event is amplified by a photomultiplier tube, which produces an electric signal. There are 25 photomultiplier tubes on each of three of the detector's faces, one normal to each axis. The output AC signal from each of the 75 photomultiplier tubes is carried by coaxial wire to a

Wilkinson Analog-to-Digital Convertor (ADC), where the signal is quantized. The number of photoelectrons on the photomultiplier tubes determines the resolution of the signal. The digital signals are recorded by the Data-Acquisition system (DAQ), from which they can be retrieved and analyzed.

Calibration is a necessary step for this system. Without a firm understanding of the significance of a given signal, data analysis will not be reliable. There are many ways the NuLat detector can be calibrated. One approach for this is muon calibration. The average energy deposition of a muon in a plastic scintillator is well-documented. By comparing the expected signals output to the photomultiplier tubes by a muon in the detector with the actual signals measured in an experimental muon event, we can determine the scaling factor necessary to translate the recorded signals to an approximation of the actual energy of the event.

To utilize muon calibration, NuLat must be able to adequately detect the signals of both muons and the IBD. However, Muons carry much more energy than antineutrinos. Therefore, if the ADC is optimized for quantization of muon signals, the neutron capture and positron signals will be too faint to be identified in data analysis. On the other hand, if it is optimized for resolution on the scale of an electron antineutrino's energy, the muon signals will saturate the digitizer and be clipped, leaving no way for us to accurately measure their amplitude, which would be detrimental to muon calibration.

The plan to circumvent this issue is to use a dual-range voltage divider network, which would allow there to be two measured data ranges. The signals from IBD will be measured and recorded normally, and the muon signals will pass through an attenuator before being recorded at a higher range.

3. Installing Attenuator Pads

This summer, I worked to build and implement attenuators for the detector, to demonstrate the potential of muon calibration. The average energy deposition of a muon in a plastic scintillator is 2MeV/cm. The NuLat detector is five cubes long, with each cube 6.35 cm long, so a single muon would deposit 57.15 MeV into the detector on average. Comparing this to the energy of an antineutrino, about 2MeV, it is clear that an attenuation on the order of one-tenth is needed^[2].

The resistance needed for a given attenuation factor depends on the inductance of the source and

the load. In this case, about 500Ω were needed. I used 470Ω resistors. I started with two boards that linked 32 RG-58 coaxial cables (from the photomultiplier tubes) with 32 connections to the transient digitizer with 220 nF ceramic capacitors. On the scrod, each path splits between a 50Ω resistor and the transient digitizer. With an added resistor between the capacitor and the transient digitizer, the pad is assembled as a voltage divider (or L-pad). I chose to use this design for its simplicity. This is the simplest passive attenuator

design, but it is not symmetric. Fortunately, the direction of the signal is known, so there is no need for the pad to be symmetric.

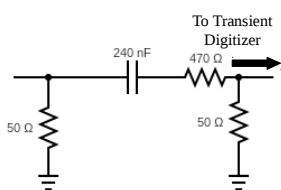


Fig. 2: Each signal's path to the scrod after the addition of the pad.

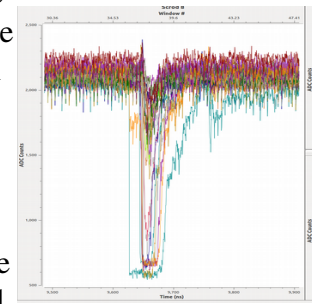


Fig. 1: The signal from a muon is cut off at the limit of the range, leaving no accurate value of its energy

I unsoldered the existing connections, adjusted the lengths of the capacitor components, and soldered in the resistors. The boards were plugged into the transient digitizer and data was collected.

In the original configuration of the detector, the $50\ \Omega$ resistors in parallel with the transient digitizer, prevents ringing from the $50\ \Omega$ characteristic impedance of the RG-58 coaxial cable. With the $470\ \Omega$ resistors added, this resistor does not terminate the ringing, so the ringing appears in our output data. However, there is another $50\ \Omega$ resistor earlier in the path of the signal, which back-terminates the ringing, so this is not a problem.

When running the detector for this data collection, the detector was set to trigger on two isolated scintillating cubes and their photomultiplier tubes. These were kept beneath the center of the detector. One cube was placed on top of the other, so that if a coincidence occurred in which both photomultiplier tubes detected a high-energy event, there was a reasonable chance that a muon had passed vertically through the detector.

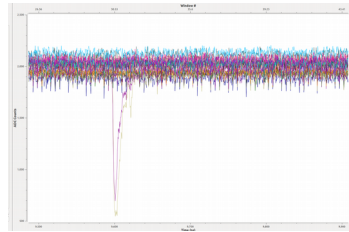


Fig. 3 a: No ringing in signal before adding attenuator pads.

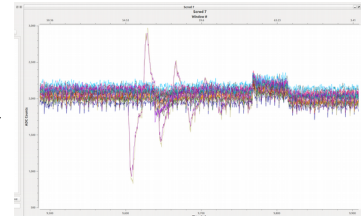


Fig. 3 b: Ringing in signal after adding attenuator pads

4. Data Analysis

To determine if the pads actually enable muon calibration, it must be determined if the attenuated muon energies collected by the attenuated detector are accurate.

We manually looked through the recorded events for instances that resembled muons. We selected some such events, each in a different vertical channel, and noted their outputs to each of the 75 photomultiplier tubes. When choosing these events, I looked for a clear signal that occurred towards the center of the timescale and for which most of the energy appeared on a single photomultiplier tube on the top face. I would also ensure that there was little to no saturation on the front and top faces.

My mentor, Dr. Vogelaar, had written a set of Fortran programs that simulated the photomultiplier tube responses from an event of user-defined energy at a user-defined location in a virtual detector with the NuLat geometry. By calculating the path of the light rays, this algorithm was designed to display the output of such a detector under ideal conditions. It would also account for the limit on a photomultiplier tube's response caused by its quantum efficiency during the photo-electric effect.

For each of the channels with an experimental event, I ran a simulation of a muon passing vertically down through the center of that channel, using $2\text{MeV}/\text{cm}$ as the average energy deposition of a muon in a plastic scintillator.

Although these events looked good when viewed on the DAQ, after the outputs were integrated and normalized, many appeared peculiar. Initially, there were many events in which there was very little light output from the attenuated faces. It was not uncommon to find events with only one non-zero photomultiplier tube response between the top and front faces. The cause of these low responses was eventually identified as an error in data collection. Upon discovery,

this mistake was promptly corrected, but among the events that had already been captured there were several fascinating cases.

Even considering the lower-voltage, it's odd that events such as 1105 have one response on the top face but none on the front, especially since the signal on the top comes from the middle of its front row. Events like these are likely caused by a muon traveling through the detector at an angle. Even though its path through the detector isn't vertical, it can still activate the trigger from the isolated cubes if it merely passes through both of them in coincidence. Due to the incline, the muon releases more of its energy toward the top than toward the front faces of the unit cube, resulting in most of the light being channeled to the top photomultiplier.

The front face output for Event 974 showed scintillator responses around the rim of its plane, but not in the center. This is likely due to the Lithium-6 doped cubes in the center of the detector. Their composition resulted in a coarse powder gradually forming within the lattice. This powder can interrupt the scintillating light from the central cubes, preventing them from sending a signal to the photomultiplier tubes, as in this case.

Event 1021 is another peculiar incident. It shows a large light output to the top face's left photomultiplier tubes and the front face's right photomultiplier tubes. This instance could be reasonably interpreted two ways. It's possible that the muon entered the detector from the top, back, left corner and exited near the bottom, front, right corner. The lack of significant response between these two points could be caused by the Lithium-doped cubes. Alternatively, there may be two separate muon events that occurred in different parts of the detector. In the first scenario, it is unlikely that this same muon could have also passed through the isolated cubes. Instead, the isolated cubes triggered on an event that did not appear in the detector but still occurred at the same time that a muon passed through the detector without entering the isolated cubes. In the second scenario, it's most likely that one of the event's muons passed through the detector and triggered the isolated cubes, while the other muon in the detector did not.

We eventually found an event that actually behaved like a muon passing vertically through the center of the detector. On the front face, the middle column showed higher-energy responses than its neighbors, although its top and bottom photomultiplier tubes captured significantly greater signals than those in between. On the left face, the numbers were higher than on the other faces, due to the lack of attenuation. Still, the values in the middle column are each significantly greater than those in the other columns. On the top face, the signal from its central photomultiplier tube is the greatest of its outputs, and the signals from the channels directly adjacent to it are each higher than most of the further channels.

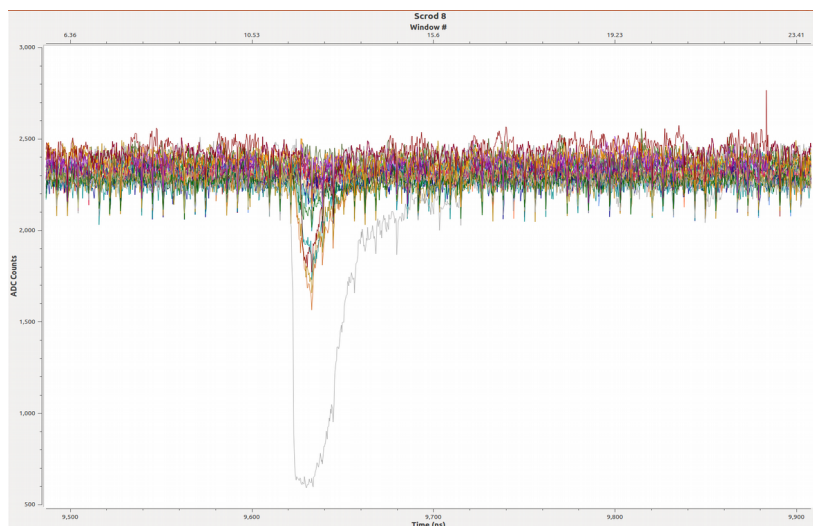


Fig. 5: A muon signal to the digitizer is attenuated, so the full height of the signal is counted. In this event, one particular photomultiplier tube receives most of the energy.

Simulated Muon: Front Face				
13	60	6184	82	10
15	66	5994	55	22
13	44	5851	59	19
10	61	5897	58	10
14	58	5522	60	18

Experimental Muon: Front Face				
9480	10947	70289	26985	13195
14763	13864	42742	5718	0
0	9191	11486	14832	8065
8841	5220	15570	0	0
0	0	40695	591	0

Simulated Muon: Left Face				
18	79	6275	95	14
9	67	5962	66	12
13	64	6092	52	12
8	72	5800	60	12
10	54	5560	66	11

Experimental Muon: Left Face				
2719	19853	158553	26588	32834
14413	6592	132180	7610	6268
4121	8782	75459	6305	3748
2130	3615	73103	1968	5733
13587	19762	148249	18052	19073

Simulated Muon: Top Face				
0	2	45	0	0
7	4	258	12	1
57	268	29061	312	62
3	15	275	6	1
0	4	42	0	0

Experimental Muon: Top Face				
0	4788	25794	3286	4835
1557	1184	25652	4258	2037
3938	17607	139291	9292	5510
11253	0	49226	143	1747
2823	13078	14781	0	25847

These experimental results are quite similar to the outputs from the Fortran simulation, when a muon's energy deposition is propagated vertically down through the central channel. The only significant difference between the two is the variation within the central columns of the front and left faces. The simulated muon loses a bit of its energy with each cube it passes through during its descent, leaving a steady gradient of scintillating light. The experimental muon's signal is also greatest at the top of each column. However, on both faces, there was much less energy collected by the photomultiplier tubes towards the middle of the column compared to the top and bottom. This is likely due to the nine Lithium-doped cubes at the center of the detector. They have a different light-yield than that of the regular cubes, so the number of photons output by them is bound to be different^[1]. Furthermore, the surprising energy of the signals from the top and bottom cubes in the central column may due to the ROL channeling of light to them through five cubes. Overall, this event is so easily comparable to the simulated muon, that it seems clear that it is a real muon event.

4. Conclusion:

Over the course of the summer, I have learned a great deal regarding particle interactions, particle detectors, and electronics. In my first week at Virginia Tech, I hadn't a clue how to

interpret the camel-hump shaped graph of an event that recorded energy from the maximum output cell and its nearest neighbor. This past week, I flipped through hundreds of events, glanced at the shape of each face's signals, and determined whether a given pulse was likely a muon event. Even during the earlier weeks of the summer, I learned a lot of skills, such as when we were figuring out how to write code representing light channeling between the cubes,

The attenuating pads served their role and reduced the amplitude of the signals enough that it was possible to witness the behavior of a muon passing through the detector. The spatial location of the muon signal could be identified, even with pads on only two of the three faces with photomultiplier tubes. The information from the unattenuated left face only served to further corroborate that the event had transpired as the other two faces' signals indicated.

Now that it is confirmed that the detector can record a muon event without losing the scale of the signal due to saturation, NuLat may begin to perform muon calibration. When successful calibration is demonstrated, then the current attenuator pads may be replaced with variable-ranged voltage dividers, to finally enable both muon calibration and detection of IBD events.

Acknowledgements

- NSF REU
- Virginia Tech Center for Neutrino Physics
- Dr. R. Bruce Vogelaar
- NuLat Colaboration
- Ryan Jewesak, Anosh Irani, and Tristan Wright (the others working in Dr. Vogelaar's lab this summer)
- The other inaugural Virginia Tech CNP REU students

Bibliography

- [1] X. Ding. "Development and calibration of NuLat, A new type of neutrino detector," 2017.
- [2] Z. Yokely. "Solar and Sterile Neutrino Physics with the Raghavan Optical Lattice," 2016.